STATUS OF X-BAND STANDING WAVE STRUCTURE STUDIES AT SLAC

V.A. Dolgashev, C. Adolphsen, D.L. Burke, G. Bowden, R.M. Jones, J. Lewandowski, Z. Li, R. Loewen, R.H. Miller, C. Ng, C. Pearson, R.D. Ruth, S.G. Tantawi, J.W. Wang, P. Wilson, SLAC, Stanford, CA 94309, USA

INTRODUCTION

Accelerating gradient is one of the major parameters of a linear accelerator. It determines the length of the accelerator and its power consumption. The SLAC two-mile linear accelerator uses 3 meter long S-band traveling wave (TW) accelerating structures. The average accelerating gradient in the linac is about 20 MV/m. This gradient corresponds to a maximum surface electric field of about 40 MV/m. An operational gradient of 40 MV/m was reported for a 1.5 m constant impedance TW structure for the SLC positron injector. This corresponds to a maximum surface field of 80 MV/m [1]. A typical operational gradient for standing wave (SW) structures of a medical linear accelerator is 30 MV/m, with surface electric fields of 130 MV/m [2] at a pulse width of several microseconds (longer than the working pulse width for SLAC TW structures). SW structures for S-band rf guns routinely operate at maximum surface fields of 130 MV/m ($\sim$2 μs pulse width) [3]. We emphasize an operational gradient with a very low fault rate in comparison to much higher gradients obtained in dedicated high gradient test structures. The operational surface fields in the above mentioned SW structures are obviously higher than in TW, S-band structures.

For the Next Linear collider (NLC) and Japanese Linear Collider (JLC), 1.8 meter long X-Band (11.4 GHz) TW structures were originally considered. Operational tests of these structures showed irreversible damage at an input power levels of $\sim$70 MW and an average gradient of about 45 MV/m (250 ns) [4]. As a consequence, an extensive experimental and theoretical program is underway at SLAC, FNAL and KEK to develop structures that reliably meet the NLC/JLC requirement of 50 MV/m loaded (65 MV/m unloaded) gradient operation [5]. This program includes testing of both TW and SW accelerating structures.

Four pairs of SW structures were built in a SLAC collaboration with KEK and LLNL. Three pairs have been tested to date and one is scheduled to be tested in May - June 2003. Design considerations, results of high power tests and future plans are discussed in this paper.

DESIGN

There are three main design requirements for a linear collider accelerator structure: the ability to sustain the working gradient, acceptable short-range wakefields, and suppressed long-range wakefields.

Other requirements for the NLC/JLC accelerating structures include: operation at 120 Hz with a 270 ns flat top pulse (after the structure is filled with rf energy); no degradation of performance during decades of operation; and less than one breakdown per 10^6 pulses per meter of structure [6, 7]. Single bunch wakefield effects limit the minimum average iris radius (a) of the structures to 4.7 mm, which is 18% of the X-band wavelength (λ= 2.62 cm).

The TW and SW structures under consideration are of the disk loaded waveguide type, are nearly constant gradient, with varying cell dimensions to produce dipole mode detuning. The structures will also include dipole mode damping.

Motivation

It is desirable for the structures to be able to operate at unloaded gradients as high as 100 MV/m, to accommodate an NLC/JLC energy upgrade above 1 TeV using the same tunnel. SW structures may prove better than TW structures in this regard. They will likely have a lower breakdown rate and less breakdown damage due to their reduced maximum surface electric fields and lower rf power absorbed per breakdown than TW structures at the same loaded gradient.

Maximum surface fields are lower in a SW structure due to the fact that the loaded gradient is equal to the unloaded gradient. However, a TW structure could be designed to reduce this difference.

The power absorbed during a breakdown is less in SW structures compared to TW structures for two reasons. It depends, first, on the lower total power fed into the structure and second, on the fact that the response of a SW structure to breakdown currents is different from the response of a TW structure.

The structure input power is determined, roughly by gradient and structure length. Reducing of the TW structure length while keeping the average iris radius 0.18λ reduces the structure efficiency. The efficiency of a SW structure does not depend on its length for the same average iris size. But this length reduction has an obvious drawback — the structure will have more couplers per meter of accelerator.

As for rf energy absorbed in the breakdown, the behavior of SW structures is very different from TW structures [8]. In TW structures during most breakdowns, a large fraction of the incident energy (up to 90%) is absorbed by the breakdown. In SW structures during most breakdowns, most of the rf power is reflected from the structure.

Design considerations

One possible scheme for a SW-based NLC/JLC linac would contain 60-80 cm long superstructures made of 3 or 4 short (20cm, 15 cell) standing wave structures. The structures in the superstructure would be separated by a 6 mm thick cutoff iris with a radius of 4.75 mm. This superstructure has 3 couplers per 60 cm of structure compared to the present NLC TW structure design that has 2 couplers per 60 cm [9]. The structure cells are azimuthially symmetric, without the Higher Order Mode (HOM) damping

Structure name		SW20a375	SW20PI	SW20a565
Iris radius, a	[mm]	3.75	4.75	5.65
Cell diameter, $2b$	[mm]	21.11	21.64	23.04
Iris thickness, t	[mm]	2.6	2.3	4.6
Iris ellipticity		1.69	1	1.48
Filling time	[ns]	120	123	118
Shunt impedance	[MΩ/m]	81.9	68.3	51.1
Q value		∼8600	∼8700	∼8400
E_{peak}/E_{acc}		2.05	2.65	2.12
RF power for $E_{acc} = 50$ MV/m	[MW]	6.0	7.2	10

Table 1: Parameters of 3 types of 20 cm long π-mode SW structures built for high power tests.

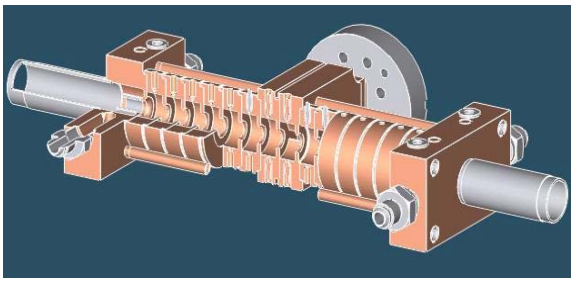

Figure 1: Cutaway view of a 15-cell π-mode SW structure with an iris radius 4.75 mm.

slots and manifolds that are in the TW structure. Long-range wakefield suppression is achieved by detuning the dipole modes within the superstructure and damping them using azimuthially symmetric cells with fundamental mode chokes and internal loads. To sufficiently damp the dipole wakefields, the structure would have one damped cell per 4 regular cells.

Test structures

To test high power performance, 4 pairs of 3 types of SW structures were built. In the test setup, a pair of SW structures is connected to the rf source using a planar 3dB hybrid. With such a connection the rf power reflected from the structures is directed to a high power load (during filling and decay time). Each 20 cm long structure has 14 cells plus a coupler cell. The coupler has two symmetrical waveguide inputs and is located in the middle of the structure. With such positioning of the coupler, the coupling from the rf source to the next-to-π resonance is suppressed. The iris radii of the three SW types are 3.65 mm, 4.75 mm and 5.65 mm. They cover the range required to detune a SW superstructure. The design parameters of these structures are shown in Table 1. Two of the structure types have elliptical iris tips to reduce the ratio of accelerating gradient E_{acc} to peak surface electric fields E_{peak}. The cutaway view of our first SW structure with a=4.75 mm is shown on Fig. 1. The three pairs of structures tested to date have sharp ($\sim$ 80 μm radius) waveguide-to-coupler cell edges. The newest pair of structures ($a = 3.65$ mm), which will be tested soon, have rounded (3 mm radius) waveguide-to-coupler iris edges to reduce the peak rf magnetic field for reasons discussed below.

HIGH POWER TEST

All SW structure testing has taken place at the Next Linear Collider Test Accelerator (NLCTA). The first pair tested have 4.75 mm iris radii and were designed with critical coupling (coupling $\beta = 1$). The structures were aggressively processed and then run at the loaded NLC/JLC gradient (at that time 55 MV/m) with a 400 ns pulse widths (150 ns structure filling plus 250 ns flat top) at the NLCTA pulse repetition rate of 60 Hz. Under these these conditions, the breakdown rate of the pair was 2-5 per hour. Video images of breakdown events viewed along the beam line axis indicated that most breakdowns were occurring in the coupler. An average of these images shows a distinct enhancement at the azimuthal positions of the waveguide-to-coupler cell edges. After the run, cold-test measurements revealed a π resonance frequency increase of ~ 0.3 MHz. Bead-pull measurements showed that most of the frequency change was in the couplers.

The second pair of structures tested was of the same type as the first but designed to have $\beta = 2$. The experience gained with the first pair prompted us to reduce the field (both magnetic and electric) in the coupler cell (relative to the field in the rest of the cells) by 15%. This was done by tuning the coupler cell frequency down a few MHz. This tuning reduced the external coupling of the structure, so that it ended up at $\beta = 1$. The pair was conditioned with ∼2000 breakdowns in three days up 55 MV/m, 400 ns, where it ran with less then breakdown per hour for ∼150 hours. The gradient was verified by a measurement of acceleration using the NLCTA electron beam. No detectable damage was found in the structure in after-test measurements.

The third pair of structures tested have the largest radii (5.65 mm) and hence the lowest shunt impedance of the three types. The structures have elliptical iris tips, an improved E_{peak}/E_{acc} ratio and a $\beta = 2$ coupling. Due to an error in coupler cell dimensions, it was not possible to reduce field in the coupler. The structure was processed to 55 MV/m, 400 ns, where the breakdown rate was 6-10 per hour. Video images again indicated that most breakdowns were in the coupler and, similar to first pair, the azimuthal

position of light from the breakdowns correlated with the position of the waveguide-to-coupler-cell edges. A shift in the π resonance of < 0.2 MHz was measured after 4300 breakdowns.

High magnetic fields

During the time of the SW structures tests, several TW structures that were processed also showed an enhancement in the coupler breakdown rate relative to that in the other cells. Measurements of breakdown induced acoustic emission near one of the TW input couplers also suggested that the breakdowns were occurring near the waveguide-to-coupler edges [10]. An autopsy of the TW structure showed that the inner edges (cell side) of the waveguide-to-coupler-cell edges were eroded [11]. Calculations showed that the surface currents peaked at the inner edge of the iris and reached ∼0.7 MA/m [12]. A simple 1D linear model of rf heating predicts a pulse temperature rise of $\sim 130^\circ$ C. It is unlikely that a temperature rise of of this size can, by itself, produce breakdowns. Some other phenomena must be present to explain the acoustic and video data, and also the large number of breakdown craters observed near the waveguide edges and the on the tips the coupler iris.

When it became apparent that the breakdowns in the couplers were preventing a further increase of the gradient in the third pair of SW structures, we continued an experimental study of the phenomena itself. These experiments showed the following properties of the coupler breakdowns:

1. The breakdown rate is determined by the input rf power and pulse width. It is roughly constant over hours and slowly increases on a longer time scale.
2. The number of pulses without breakdown is roughly independent of the pulse repetition rate.
3. The breakdown rate has a clear correlation with the pulse temperature rise as calculated using a simple model of rf pulse heating. The breakdown rate grows almost exponentially with the temperature as seen in Fig. 2. On a linear scale, it appears like the breakdown rate has a threshold. The threshold temperature varies from 60 to 150° C for the different accelerating structures.

Discussion

Mechanical damage due to pulse heating is discussed in [13, 14] and may be related to the observed breakdown characteristics. The model described in [15] suggests that the mechanical fatigue accumulates with each pulse and (after certain number of pulses) macroscopic change occurs (similar to creation of a dislocation). This model is supported by the experimental data on coupler breakdowns in SW and TW structures with an additional assumption that this macroscopic change triggers the rf breakdown. The mechanism of the surface heating also needs verification, since other effects, like single surface multipactor discharge in strong rf magnetic fields could also increase surface the temperature. Also, more recent TW structure

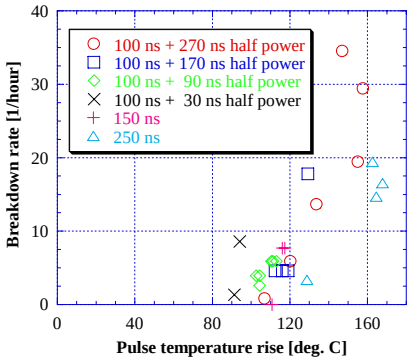

Figure 2: Measured breakdown rates for the SW20a565 structure *vs.* calculated pulse temperature rise on the waveguide-to-coupler iris edges for different shapes of the input rf pulse.

tests showed that some couplers did not breakdown even when the predicted pulse temperature rise was well above 100° C. The absence of breakdown in such cases might be explained by relatively small (∼1 MV/m) electric field on the iris edge of the coupler without breakdowns in comparison with fields (∼10 MV/m) in couplers with breakdowns [12].

SUMMARY

Three pairs of SW structures have been tested to date. The performance of two of them was limited to gradients lower than 55 MV/m by breakdowns in the couplers. These breakdowns may be related to the high rf magnetic and moderate rf electric fields on the sharp edges at the waveguide-to-coupler cell opening. Couplers for a new set of structures have been designed to reduce the pulse temperature rise to below 20° C. These structures will be high power tested in May-June 2003.

Despite the potential for coupler breakdowns, one of SW structure pairs tested ($a = 4.57$ mm) did meet NLC/JLC gradient and breakdown rate requirements and had no measurable damage.

REFERENCES

[1] J. E. Clendenin, *et al.*, Part. Accel. **30**, 85 (1990).
[2] C. J. Karzmark, *et al.* " Medical Electron Accelerators," McGraw-Hill, Inc., New York, 1993.
[3] D. T. Palmer *et al.*, SLAC-PUB-7422.
[4] C. Adolphsen *et al.*, TUE01, LINAC2000, 2000, Monterey, CA.
[5] J. W. Wang *et al.*, TH464, LINAC02, 2002, Gyeongju, Korea.
[6] "2001 Report on The Next Linear Collider," SLAC-PUB-R-571, Snowmass, Colorado, 2001.
[7] "NLC Newsletter," July, 2002.
[8] V. A. Dolgashev, *et al.*, FPAH057, PAC2001, Chicago, IL, 2001, pp. 3807-3809.
[9] Z. Li, *et al.*, WPAG027, this conference.
[10] J. Frisch *et al.*, TH484, LINAC02, Gyeongju, Korea, 2002.
[11] F. Le Pimpec *et al.*, MO486, LINAC02, Gyeongju, Korea, 2002.
[12] V. A. Dolgashev, TPAB032, this conference.
[13] O. A. Nezhevenko, PAC97, Vancouver 1997, p.3013.
[14] D. P. Pritzkau, "RF Pulsed Heating," SLAC-Report-577, Ph.D. Dissertation, Stanford University, 2001.
[15] V. F. Kovalenko *et al.*, "Thermophysical Processes and Electrovacuum Devices," Moscow, SOVETSKOE RADIO (1975), pp. 160-193.